Nanoscale Advances

ROYAL SOCIETY OF CHEMISTRY

PAPER

View Article Online
View Journal | View Issue

Cite this: *Nanoscale Adv.*, 2022, **4**, 2857

Morin encapsulated chitosan nanoparticles (MCNPs) ameliorate arsenic induced liver damage through improvement of the antioxidant system and prevention of apoptosis and inflammation in mice†

Sanchaita Mondal,[ab] Sujata Das,[a] Pradip Kumar Mahapatra[b] and Krishna Das Saha *[a]

Chronic exposure to arsenic over a period of time induces toxicity, primarily in the liver but gradually in all systems of the body. Morin hydrate (MH; 2′,3,4′,5,7-pentahydroxyflavone), a potent flavonoid abundantly present in plants of the Moraceae family, is thought to be a major bioactive compound that may be used to prevent a wide range of disease pathologies including hepatotoxicity. Therapeutic applications of morin (MOR) are however seriously constrained because of its insolubility, poor bioavailability, high metabolism and rapid elimination from the human body. Nanoformulation of MOR is a possible solution to these problems. In the present study we investigated the effectiveness of morin encapsulated chitosan nanoparticles (MCNPs) against arsenic induced liver damage in mice. MNCPs with an average diameter of 124.5 nm, a zeta potential of +16.2 mV and an encapsulation efficiency of 78% were prepared. Co-treatment of MOR and MCNPs by oral gavage on alternate days reduced the serum levels of AST, ALT, and ALP that were elevated in arsenic treated mice. The efficiency of MCNPs was found to be nearly 4 times higher than that of free MOR. Haematological and serum biochemical parameters including lipid profiles altered by arsenic were normalized following MCNP treatment. Arsenic deposition was lowered in the presence of MCNPs. Administration of MCNPs markedly inhibited ROS generation and elevated MDA levels in arsenic exposed mice. The level of hepatic antioxidant factors such as nuclear Nrf2 (Nrf2), superoxide dismutase (SOD), catalase (CAT), glutathione (GSH), GSH peroxidase (GPx), glutathione-S-transferase (GST), heme oxygenase-1 (HO-1), and NADPH quinone oxidoreductase 1(NQO1) were markedly enhanced in the arsenic + MCNP group. Treatment by MCNPs prevented the arsenic induced damage of tissue histology. Also, MCNPs suppressed the arsenic induced pro- and anti-apoptotic parameters and attenuated the level of inflammatory mediators. Our data suggest that MCNPs are good hepatoprotective agents compared to free morin against arsenic induced toxicity and the protective effect results from its strong antioxidant, antiapoptotic and anti-inflammatory properties.

Received 17th March 2022
Accepted 30th April 2022

DOI: 10.1039/d2na00167e

rsc.li/nanoscale-advances

Introduction

Arsenic, a naturally occurring metalloid, exerts genotoxic and carcinogenic effects on living organisms in different parts of the world.[1] Applications of the derivatives of arsenic as herbicides, insecticides, rodenticides, food preservatives, and fossil fuels are drastically contaminating drinking water. Arsenic induced toxicity has been reported to be associated with liver dysfunction, renal failure, dermatitis, cardiovascular diseases, peripheral neuropathy, diabetes mellitus and varieties of cancers.[2] Liver disease is a major risk of environmental arsenic exposure worldwide. The liver is the primary target organ for the metabolism of arsenicals.[1] The major metabolic pathway of inorganic arsenic in humans is its methylation in the liver. Arsenite salt may exert its toxicity through reactions with thiols in cells and generation of reactive oxygen species (ROS) during their metabolism in cells.[3]

The serum level of liver damage markers such as alanine amino transferase (ALT), aspartate amino transferase (AST) and alkaline phosphatase (ALP) are elevated in arsenic induced liver toxicity.[4] It is demonstrated that arsenic intoxication leads to the generation of reactive oxygen species (ROS), along with the rapid depletion of antioxidant enzymes such as superoxide dismutase (SOD) and catalase.[3] Nrf2, a major redox regulator,

[a]*Cancer Biology and Inflammatory Disorder Division, CSIR-Indian Institute of Chemical Biology, 4, Raja S.C. Mullick Road, Kolkata-700032, West Bengal, India. E-mail: krishna@iicb.res.in; dassahakrishna@gmail.com*

[b]*Department of Chemistry, Jadavpur University, 188, Raja S.C. Mullick Road, Kolkata-700032, West Bengal, India*

† Electronic supplementary information (ESI) available. See https://doi.org/10.1039/d2na00167e

remains attached to the kelch-like ECH-associated protein-1 (Keap1) in the cytoplasm, and is inactive in this bound state. Nrf2 is dissociated from Keap1 under oxidative stress and is thus activated.[5] There is a translocation of the activated Nrf2 to the nucleus where it interacts with the antioxidant response element (ARE) and promotes the expression of different anti-oxidant enzymes such as catalase (CAT), superoxide dismutase (SOD), glutathione (GSH), GSH peroxidase (GPx), glutathione-S-transferase (GST), heme oxygenase-1 (HO-1), NADPH quinone oxidoreductase 1(NQO1), *etc.* Antioxidant enzymes and non-enzymatic anti-oxidant factors are affected in arsenic induced liver injury.[4]

Arsenic induced organ injury results in an inflammatory response with the production of inflammatory mediators like cytokines TNF-α, IL-1β and IL-6, NO, COX-2 *etc.* Nuclear transcription factor-kB (NF-kB) remains inactive through attachment with its inhibitor called IkB in the cytosol. Dissociation of NF-kB from IkB leads to its activation following its translocation to the nucleus, where it regulates the transcription of pro-inflammatory genes. Transforming growth factor-β plays a key role in the progression of liver diseases including liver toxicity. NLRP3 inflammasome activation occurs in severe liver injury with the increased expression of caspase-1, IL-1β *etc.*

In arsenic induced hepatic injury, oxidative stress mediated DNA damage and hepatocyte apoptosis is a core event (Nithyananthan *et al.*, 2020). Therefore, the inhibition of hepatocyte apoptosis is one of the indices to investigate the efficacy of liver protective drugs (Kim *et al.*, 2004; Ozaki, 2019).

Several studies report on hepatic protection by plant polyphenols against arsenic induced organ toxicity.[6] Morin hydrate (MH; 2′,3,4′,5,7-pentahydroxyflavone), a yellowish pigment and a potent flavonoid present in various edible fruits and vegetables, belonging to the Moraceae family, is used as a herbal medicine. Morin has hepatoprotective activity.[7] The protective efficacy of morin is mainly attributed to its anti-oxidant and anti-inflammatory properties and also the unique structural feature that assists morin to interact with nucleic acids, enzymes and proteins.[7]

But like other flavonoids, morin shows low water solubility in its free form, a high rate of metabolism and rapid elimination from the human body.[8] Moreover, it undergoes degradation in water or oxidation, with a consequent loss in activity. All these factors contribute to a lack of long-term stability and to poor vascular and oral bioavailability that drastically reduce the effectiveness of the compound which depends on preserving the stability, bioactivity and bioavailability. Therefore, the development of new strategies to overcome the drawbacks associated with MOR can provide a relatively low cost and indigenous therapeutic lead in the treatment of liver ailments.

Chitosan, a natural polysaccharide derivative of chitin, is a poly-cationic linear polymer that has high potential to encapsulate natural ingredients. Chitosan is biocompatible, non-toxic and biodegradable, and has good bio-adhesive properties, making it capable of *in vivo* use through oral, intraperitoneal or intravenous administrations. Additionally, chitosan nanoparticles (CNPs) can be easily prepared based on ionic gelation between positively charged chitosan polymer tripolyphosphate (TPP) anions. Therefore, it seems that CNPs have a high capacity for delivering naturally available water insoluble compounds like morin.

Very recently, polymeric nanoparticles have been increasingly used as a potential drug delivery system. The notable advantage of polymeric nanoparticles is that they can be easily prepared by different chemical methods. The topological and morphological control of nanoparticles is crucial in order to accomplish specific applications in emerging areas of nanotechnology. The high surface area and internal void space present in the nanoparticles can make them an ideal medium as a drug delivery vehicle.[9] In particular, the structures of polymeric nanoparticles are very attractive because of the unique topology that offers low density, high surface area, high pore volume, narrow pore size distribution, non-toxic nature and biocompatibility. In this context, nanotechnology can play a pivotal role in the development of nanomaterials that can be used for therapeutic applications in various inflammatory diseases.[10]

So, in this study, we have synthesized and characterized morin encapsulated chitosan nanoparticles (MCNPs) and evaluated their hepatoprotective role, potential to ameliorate oxidative stress, and inhibit apoptosis and inflammation.

Materials and methods

Chemicals

Morin hydrate (purity ≥ 99.0%), chitosan (low MW, extrapure), dichloromethane (DCM) and poly-(vinyl alcohol) (PVA), were purchased from Sisco Research Laboratories (Gurugram, India); erlotinib hydrochloride (purity ≥98.0%), all primary and secondary antibodies and sodium TPP were purchased from Sigma-Aldrich, MO, USA. Assays kits for the detection of serum ALT, AST, AP, SOD, catalase, GPx, HDL, LDL, triglyceride (TG), and total cholesterol (TC) were purchased from ARKRAY Healthcare Pvt. Ltd (Surat, India). IL-1β, IL-6, TGF-β and TNF-α were measured by using ELISA kits from the R & D system (MN, USA). All other chemicals were available commercially and of a high degree of purity.

Preparation and characterization of MCNPs

Morin encapsulated chitosan nanoparticles (CNPs) were synthesized by using the ionic gelation method.[11] Briefly, a desired amount of chitosan dissolved in acetic acid (1%) was mixed with a certain amount of morin hydrate solution which was dissolved in slightly alkaline double distilled water under magnetic stirring (1000 rpm) at room temperature. After 5 min of stirring, TPP solution was added dropwise to the mixture to form nanoparticles. For the preparation of nanoparticles with the highest encapsulation efficacy, chitosan, morin and TPP were used in a 3 : 5 : 5 ratio according to Bardania *et al.* The solution of the prepared nanoparticles was centrifuged at 10 000 rpm for 10 min. The supernatants were used to determine the amount of morin encapsulated into the nanoparticles. The CNPs packed with morin have been examined for characterization in terms of Fourier transform IR spectroscopy, size

distribution, morphological characteristics, zeta-potential, shape, the efficacy of drug encapsulation, the percentage of drug loading and release of the *in vitro* product.

Encapsulation efficiency and drug loading

NPs (5 mg) were soaked in 5 ml of phosphate buffer for 30 min. The solution was centrifuged at 4000 rpm at 4 °C for 40 min, and the precipitate was washed twice with fresh solvent to remove the unconjugated drug. Using a UV spectrophotometer (JASCO V-730, spectrophotometer, Tokyo, Japan) at λ_{max} values of 270 and 395 nm, the clear supernatant solution was analyzed for unencapsulated morin. Morin standard curves were obtained by plotting the concentration against the absorbances from 10 to 50 mg ml^{-1}.

The percentages of drug loading and entrapment efficiency were calculated by using the following formula:

Encapsulation efficiency (%) = (The total amount of drug released from the lyophilized MCNPs/Amount of drug initially taken to synthesize the MCNPs) × 100.

Drug loading (%) = (Amount of drug found in the lyophilized MCNPs/Amount of lyophilized MCNPs) × 100.

Particle size & zeta potential measurement

A Zetasizer 3000 HSA (Malvern Instruments, Malvern, UK) was used to measure the particle size, distribution and zeta potential. For the DLS measurements, NPs were diluted with double distilled water, and 500 μl was loaded into the cuvette and transferred to zeta sizer cells for zeta potential measurement.

Fourier transform infrared spectroscopy

To identify the various functional groups present in morin, chitosan and MCNPs, FT-IR was performed. Morin, chitosan and the synthesized NPs were centrifuged and lyophilized earlier; and the powders of all three were analysed using the IR spectra recorded using a PerkinElmer FT-IR spectrometer (MA, USA) in the absorbance mode to interpret the presence of different functional groups.

Atomic force microscopy (AFM)

5 μL of the samples (1 mM) were deposited onto a freshly cleaved muscovite ruby mica sheet (ASTM V1 Grade Ruby Mica from MICAFAB, Chennai) for 5–10 minutes, and then the sample was dried by using a vacuum dryer. AAC mode AFM was performed using a Pico plus 5500 AFM (Agilent Technologies USA) with a piezo scanner with a maximum range of 9 μm. Micro-fabricated silicon cantilevers 225 μm in length with a nominal spring force constant of 21–98 N m^{-1} from nanosensors were used. The cantilever oscillation frequency was tuned to the resonance frequency. The cantilever resonance frequency was 150–300 kHz. The images (256 by 256 pixels) were captured with a scan size between 0.5 and 5 μm at a scan rate of 0.5 lines per s. The images were processed by flattening using Pico view1.4 version software (Agilent Technologies, USA). Image analysis was done through Pico Image Advanced version software (Agilent Technologies, USA).

Transmission electron microscopy (TEM)

A freshly prepared solution of the MCNPs in double distilled water was placed on a TEM grid (300-mesh carbon-coated Cu grid). The samples were allowed to dry in air at room temperature for a few hours before the measurements were recorded.

In vitro drug release studies

The MCNPs were solubilized in a phosphate-buffered saline (PBS) medium (1 M, NaCl = 8 gm, KCl = 0.2 gm, Na_2HPO_4 = 1.44 gm, and KH_2PO_4 = 0.24 gm were dissolved in double distilled water and the pH was adjusted to 7.4). To study the *in vitro* release kinetics, the MCNPs (10 mg) were filled in a dialysis bag with a cut off size of 5 kDa, put in 200 ml of PBS of pH 7.4 and stirred at 100 rpm for 4 days. 2 ml of the buffer solution was removed after a fixed time interval and replaced with fresh buffer. Using a UV-visible spectrophotometer (JASCO V-730 spectrophotometer, Tokyo, Japan) at 270 and 395 nm, respectively, the release of drugs has been tested. The experiments were repeated thrice, and the average values were evaluated.

Animals

Male BALB/c mice of 6–8 weeks weighing 20–22 gms were procured from the animal house division of our institute (CSIR-Indian Institute of Chemical Biology, Kolkata) and fed with standard chow diets and drinking water. The animals were kept at 22–24 °C temperature, 50–60% humidity, and subject to light and dark cycles of 12 : 12 h. All animal procedures were performed in accordance with the Guidelines for Care and Use of Laboratory Animals of CSIR-Indian Institute of Chemical Biology Animal Ethics Committee and approved by the Animal Ethics Committee of CSIR-Indian Institute of Chemical Biology.

Dose selection of MOR and MCNPs

After acclimatization for 7 days, each group of mice was treated with 0 mg, 100 mg, 200 mg, and 400 mg kg^{-1} body weight of MOR or 75 mg, 150 mg, 300 mg kg^{-1} body weight of MCNPs every alternate day upto 28 days by oral gavage. AST and ALT were measured at different time intervals. Doses of MOR or MCNPs that did not elevate the level of AST or ALT were selected for experimental study.

Survival study

Mice were challenged with different doses of arsenic for 30 days followed by treatment without or with different doses of MOR or MCNPs. The number of mice that survived on day 30 was monitored and the % survival of mice was calculated.

Experimental design

The experimental plan of this study was as follows: Group I: mice were exposed to arsenic (40 mg L^{-1}) only *via* drinking water for 30 days. The arsenic exposed mice were orally given 0 mg, 50 mg, 100 mg, and 200 mg kg^{-1} body weight of MOR (group II–V) and 25, 50, and 100 mg kg^{-1} body weight of MCNPs (group VI–VIII). Both MOR and MCNPs were given on every

alternate day by suspending them in 0.1% Tween 80 in PBS starting from day 2 to 28 of arsenic exposure. Blood was drawn by tail vein puncture at different time points from each group of mice, for serum analysis. The mice were sacrificed after 30 days and the liver sections were collected for histology, immunohistochemistry and western blot analysis. For biochemical testing, one part of the liver was stored in a −80 °C freezer, and the other part was cut and placed in a bottle containing 10% neutral-buffered saline for performing histopathological analysis the next day.

Measurement of serum ALT, AST, HDL, LDL, TG, TC, TC, TG, LDL, HDL, uric acid, creatinine, and MDA

The blood samples were obtained by tail-vein puncture and kept at 4 °C undisturbed o/n. The samples were centrifuged the next day(1100× g, 10 min, 4 °C) to obtain the serum from the experimental groups. Serum AST, ALT, ALP, HDL, LDL, TG, TC, SOD, GPx and catalase activities were calculated according to the instruction brochure provided with the commercial assay kits.

Assessment of arsenic deposition in organs

A simple spectrophotometric method has been followed for the determination of arsenic in various organs of the murine samples. The method is based on the reaction of arsenic(III) with potassium iodate in an acid medium to liberate iodine. This liberated iodine bleaches the red color of rhodamine B. A calibration curve was prepared by adding 2 ml of potassium iodate and 1 ml of HCl to an aliquot of a working standard solution containing 1.0–10.0 μg of arsenic in a 25 ml calibrated flask and the mixture was shaken gently. This was followed by addition of 2 ml of 0.05% rhodamine-B. The solution was kept for 15 min and made up to the mark with deionised water. The decrease in absorbance at 550 nm is directly proportional to the arsenic(III) concentration and obeys Beer's law.[12] Then a measured amount of the liver and spleen samples were taken in a 15 ml polypropylene tube in the presence of 3 ml of nitric acid (61%). The tubes were capped properly and incubated at 80 °C for 48 h, followed by cooling for 1 h to room temperature. After cooling, 3 ml of hydrogen peroxide (30%) was added to each tube, followed by incubation at 80 °C for 3 h. After suitable dilution of the digested materials with ultrapure water, the levels of arsenic in the samples were determined. The sample solution (1 ml) obtained after digestion of the tissue was mixed with 2 ml of KIO_3 and 1 ml of HCl. And the mixture was shaken gently followed by addition of 0.1% rhodamine-B. The solution was kept for 15 min. The absorbance was measured at 550 nm.

Determination of ROS

The liver samples (200 mg each) were homogenized (1 : 10 w/v) in Tris–HCl buffer (40 mM, pH = 7.4, 0 °C). One hundred mililiters of the tissue homogenate was mixed with 1 ml of Tris–HCl buffer and 5 μl of 2,7-dichlorofluorescein diacetate solution (10 mM). The mixture was incubated for half an hour at 37 °C. Finally, the sample's fluorescence intensity was measured using a spectrofluorometer at 480 and 525 nm wavelengths of excitation and emission.

Estimation of lipid peroxidation levels in the liver

The level of lipid peroxidation in liver tissues was measured as the amount of thiobarbituric acid reactive substances (TBARS).[13] Thiobarbituric acid reacts with MDA (malondialdehyde), a major lipid oxidation product to form a red product (TBARS) that can be detected colorimetrically at 532 nm or fluorometrically at Ex/Em 532/553 nm. Briefly, supernatants of tissue lysate were mixed with an equal volume of TCA-BHT (BHT = butylated hydroxytoluene) in order to discard proteins. BHT stops further sample peroxidation during the experimental process. After centrifugation (1000 g, 10 min, 4 °C), 200 ml of the resulting supernatant was mixed with 40 ml of HCl (0.6 M) and 160 ml of thiobarbituric acid (TBA) 20% dissolved in Tris. The mixture was heated at 80 °C for 10 min, and after cooling at room temperature, the absorbance was measured at 530 nm and TBARS values were calculated and expressed in nmol mg^{-1} protein.

Estimation of SOD, GSH, and catalase

The blood samples were obtained by tail-vein puncture and kept at 4 °C undisturbed o/n. The samples were centrifuged the next day(1109× g, 10 min, 4 °C) to obtain the serum from the experimental groups. Serum, SOD, GSH and catalase activities were calculated according to the instruction brochure provided with the commercial assay kits.

Histological evaluation

The fixed liver tissues in 10% neutral buffered formalin (NBF) were embedded in paraffin, thinly sectioned, de-paraffinated and rehydrated using the standard histology procedure. Various pathological changes were assessed by using hematoxylin and eosin stains.

Assessment of serum cytokines

The blood samples were isolated at different time points as mentioned above, and the serum levels of TNF-α, IL-1β, TGF-β and IL-6 were determined using the commercially available ELISA kit according to the manufacturer's instruction and guidelines (R&D Systems, MN, USA).

Tissue distribution study

All mice were fasted overnight and were fed only water before the experiments. Standard stock solutions of MOR and MCNPs (1 mg ml^{-1}) were prepared by dissolving specific amounts of the drug in ethanol. After oral administration of MCNPs, the mice were sacrificed at 2, 6, 12, 24, 48, and 72 h. Various tissues (liver, lung, kidney, and spleen) were collected and washed with 0.9% NaCl to remove extra blood and contents. After blotting them with filter paper, 1 mg equivalent from the tissues was weighed and homogenized in 1 ml of 0.9% NaCl. Then, 100 μL of it was used as the tissue sample. The blood samples were drawn from the tail vein and coagulated for half an hour in an MCT tube. The blood samples were centrifuged at 2000 rpm for 10 min (4 °C), and the serum was obtained from the supernatant. Then, 100 μL of the serum was

used as the sample. The tissues were stored at −80 °C for further use.[14]

Western blot analysis

The dissected tissues frozen in liquid nitrogen were disrupted using a homogenizer and RIPA lysis buffer and then centrifuged. Protein concentrations in the supernatant of the tissue lysate were assessed using the Bradford method.[15] SDS-PAGE was carried out on an acrylamide gel to separate the proteins, which were then transferred to a polyvinylidene difluoride membrane. The membrane is blocked with 10% skimmed milk or 5% BSA and incubated overnight with primary

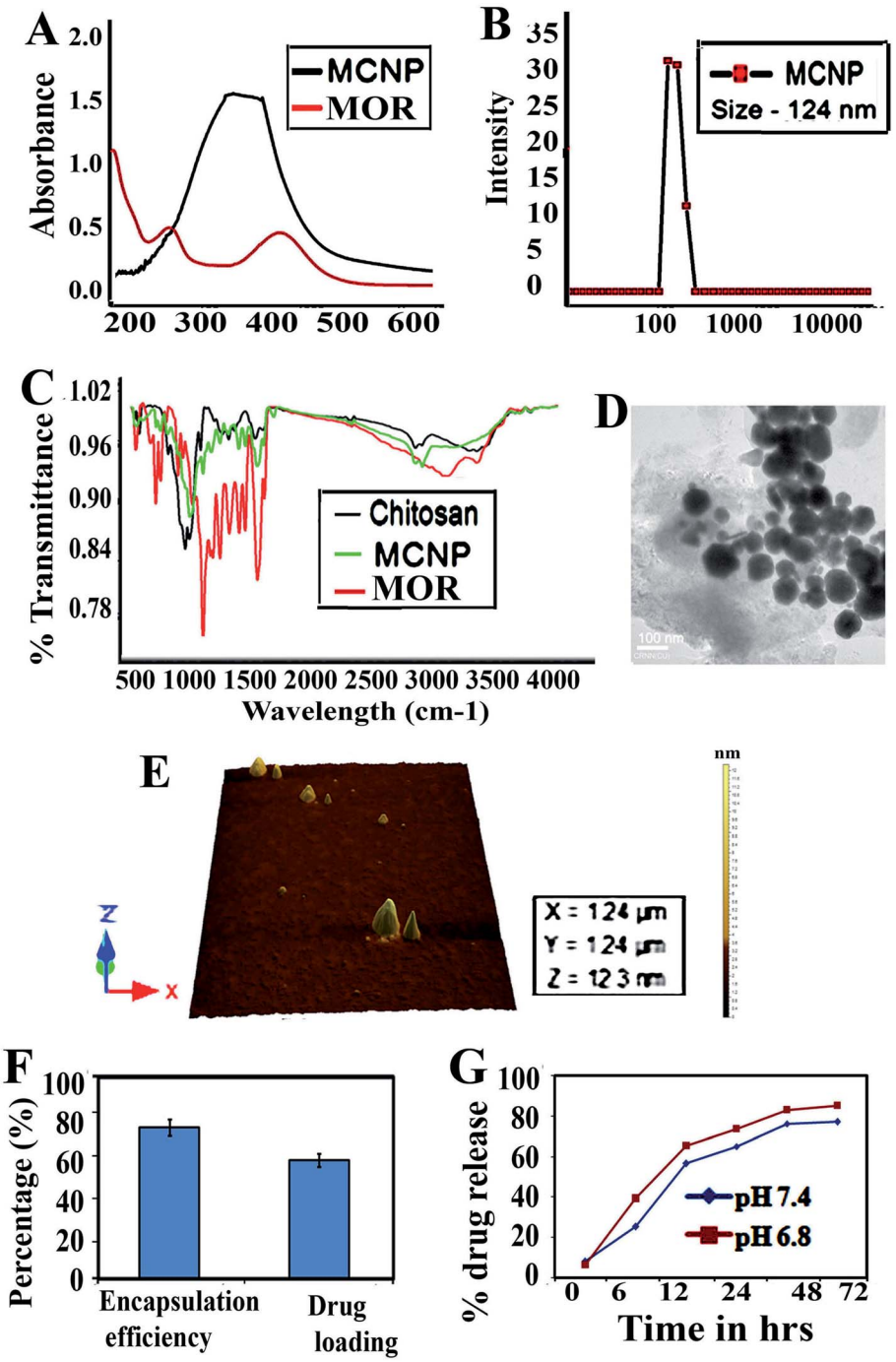

Fig. 1 Characterization of morin loaded chitosan nanoparticles. (A) UV-visible spectra of morin and MCNPs. The red line shows the spectra of morin and the black line shows the spectra of MCNPs. (B) Particle size distribution from differential light scattering (DLS) with MCNPs. (C) Fourier transform infrared spectroscopy (FTIR) spectra of Morin, chitosan, and MCNPs. (D) TEM images of MCNPs. (E) MCNP particle surface topology determination using atomic force microscopy (AFM). The acquired images were analyzed using scanning probe microscopy (SPM) tools for the laboratory study. (F) Encapsulation efficiency percentage and drug-loading percentage of MCNPs. (G) Percentage of release of morin from MCNPs over a time period of 0–72 h. The result is the mean ± standard deviation (SD) from triplicate independent experiments.

antibodies of different proteins and β-actin (1 : 1000; Santa Cruz, CA, USA), and the next day, after washing the membrane 3 times with wash buffer, it was incubated with the alkaline phosphatase conjugated secondary antibody for 2 h. At last, protein expressions were detected using NBT/BCIP solution.

Immunohistochemical analysis

Paraffin-embedded blocks of liver tissues were cut into thin sections and mounted onto slides. Xylene was used to deparaffinize the liver sections, and various concentrations of alcohol were used to rehydrate the tissues. The antigen retrieval step was performed using sodium citrate buffer (10 mM sodium citrate, 0.05 percent between 20, pH = 6.0) for 20 min in a water bath at 100 °C. A 5% solution of BSA was used for blocking in Tris-buffered saline (TBS, 20 mM Tris–HCl, pH 7.4 containing 150 mM NaCl) for 2 h. For permeabilization, the tissue sections were washed with TBST (Tris-buffered saline, 0.1% Tween 20). Finally, at a dilution of 1 : 500 at 4 °C overnight in a humidified chamber, the sections were incubated with the primary antibody. The tissue sections were washed with 1× TBS and incubated with 1 : 400 dilution of Alexa fluor 555 (red) and Alexa fluor 488 (green) conjugated secondary antibodies for 2 h at room temperature. The nucleus was visualized by using the Hoechst (Invitrogen, CA, USA) stain. The images were observed using an automated laser scanning confocal microscope (Olympus FV10i, Shinjuku, Tokyo, Japan).

Statistical analysis

All data from at least three experiments with replicates were expressed as the mean standard deviation (SD). Using

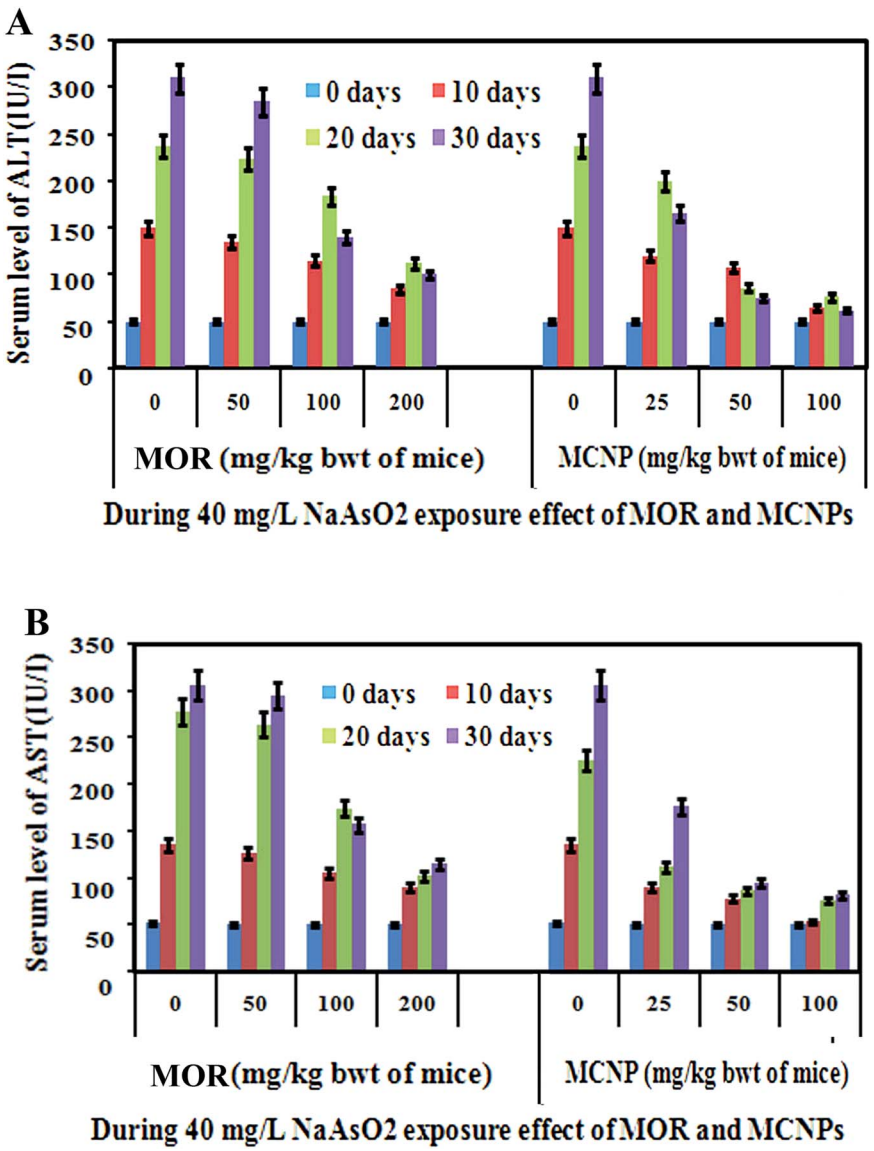

Fig. 2 Effect of Morin (MOR) and MCNPs on arsenic induced elevation of ALT and AST. Morin (MOR) and MCNP levels with the duration of its exposure. Mice were treated with indicated doses of morin (MOR) and MCNPs during arsenic exposure. Data show one of the three representative experiments ± SD.

GraphPad Prism software (CA, USA), statistical significance and differences between the control and five other treatment groups were analyzed using a one-way analysis of variance.

Results

Characterization of MCNPs

Morin encapsulated chitosan nanoparticles (MCNPs) prepared by the ionic gelation method were characterized. Fig. 1A shows the UV-vis absorbance spectra of morin and MCNPs. DLS shows that the MCNPs have a diameter of 124 ± 1.5 nm (Fig. 1B), with a polydispersity index value of 0.18, suggesting low polydispersity. The zeta potential value of the MCNPs is −28.4 ± 0.39 mV, which tended to stabilize the NP suspension. Fourier transform IR (FTIR) demonstrates the compatibility between MOR, chitosan and morin loaded chitosan nanoparticles as shown in Fig. 1C. The FTIR spectra covers the region from 4000 cm^{-1} to 500 cm^{-1}. The significant peaks assigned for MOR, chitosan and MCNPs confirm the presence of different functional groups. The strong, broad peak at 3400 cm^{-1} is due to O–H (stretching), while a sharp peak at 1650 cm^{-1} corresponds to the presence of aromatic ester (C═O) and alkene (C═C) groups and another strong, sharp peak at 1200 cm^{-1} indicates C–OH stretching. The strong, sharp peak at 3100 cm^{-1} is due to O–H (stretching), and a sharp peak at 1647 cm^{-1} corresponds to the presence of alkene (C═C) groups, and a sharp peak observed at 1160 cm^{-1} is the indication of C–OH (stretching) in chitosan. The MCNP shows a peak at 3100 cm^{-1}, which suggests that the O–H groups of MOR and chitosan are conserved. Small peaks at 1645 cm^{-1} and 1120 cm^{-1} denote the conservation of the alkene (C═C) and ester (C═O) groups and the C–OH bond of MOR and chitosan in the MCNP. Atomic force microscopy (AFM) and transmission electron microscopy (TEM) reveal that the surface topology of MCNPs is spherical, and they are uniformly distributed without aggregation. The size of MCNPs ranges between 100 and 200 nm, as shown in Fig. 1D and E.

The encapsulation efficiency of MOR is 73 ± 2.5%. The formulation optimized for spherical shaped NPs results in a high drug encapsulation efficiency. The drug loading for MOR is 58 ± 3.3% (Fig. 1F). The drug release kinetics of morin-loaded chitosan NPs are shown in (Fig. 1G). The nanoparticles release 53% MOR in 24 h. A constant slow release of MOR is observed for 4 days, but the maximum release is observed at 72 h which is 86.5%.

Effect of MOR and MCNPs on AST, ALT, body weight, hematological parameters, kidney function markers and lipid profiles

Non-toxic doses of MOR and MCNPs in mice were determined by measuring the effect of their different doses on the serum level of AST and ALT. Up to 200 mg kg^{-1} of MOR and 100 mg kg^{-1} of MCNPs given orally on alternate days up to 30 days did not raise the serum level of AST and ALT (ESI Fig. 1A and B).† However, the level of AST and ALT increased following treatment with 400 mg kg^{-1} body weight of MOR and 200 mg kg^{-1} body weight of MCNPs. So, the effect of MOR and MCNPs on arsenic induced toxicity was investigated using maximum doses of 200 mg kg^{-1} and100 mg kg^{-1} respectively.

The serum level of AST and ALT increased with time in arsenic exposed mice (40 mg L^{-1}). Treatment of MOR (50, 100 and 200 mg Kg^{-1} bwt) and MCNPs (25, 50, and 100 mg Kg^{-1} bwt) on alternate days during the arsenic exposure dose dependently lowered the levels of AST and ALT (Fig. 2A and B). The effect of 25 mg kg^{-1} and 50 mg kg^{-1} of MCNPs was comparable with 100 mg kg^{-1} and 200 mg kg^{-1} bwt of MOR respectively. Thus, the potency of MCNPs was nearly four times higher than that of MOR and the optimum effect was observed with 50 mg kg^{-1} of MCNPs and 200 mg kg^{-1} bwt of MOR.

Arsenic exposure suppressed the increase of body weight, lowered the level of RBCs, hemoglobin (Hb), platelets (PLTs), HDL (good cholesterol) and increased WBCs, LDH, kidney function markers such as uric acid and creatinine, and lipid markers such as cholesterol, triglycerides, and LDL (bad cholesterol). A high LDH level is the indication of tissue damage. Treatment of mice with 50 mg kg^{-1} bwt MCNP and 200 mg kg^{-1} bwt of MOR reversed the arsenic induced

Table 1 Effect of oral administration of MOR and MCNPs on haematological parameters[a]

Parameters	Control Group	Arsenic (40 mg L^{-1}) treated mice	Arsenic + MOR (200 mg kg^{-1}) treated mice	Arsenic + MCNPs (50 mg kg^{-1})
Body weight gain (gm)	0.61 ± 0.04	0.34 ± 0.05	0.46 ± 0.02	0.39 ± 0.04
RBC: no. of cells (10^6/μL)	7.5 ± 0.82	5.6 ± 0.54	6.5 ± 0.44	7.1 ± 0.38
WBC: no. of cells (10^3/μL)	12.4 ± 0.06	15.8 ± 0.22	14.1 ± 0.54	13.5 ± 0.42
Hb (gm dl^{-1})	12.9 ± 0.42	10.1 ± 0.3	11.9 ± 0.23	12.5 ± 0.31
PLT (10^3/μL)	542 ± 34.2	422 ± 37.6	502 ± 26.7	526 ± 18.1
LDH (U/L)	391 ± 26.3	751 ± 41.6	481 ± 24.6	415 ± 21.8
Uric acid (mg dL^{-1})	2.79 ± 0.62	4.66 ± 0.71	3.12 ± 0.22	2.88 ± 0.21
Creatinine (mg dL^{-1})	0.45 ± 0.04	2.6 ± 0.16	1.1 ± 0.08	0.62 ± 0.08
Cholesterol (mg dL^{-1})	135 ± 9.8	287 ± 25.2	159 ± 15.2	142 ± 8.5
TG (mg dL^{-1})	82.1 ± 7.7	159 ± 11.8	91.4 ± 6.5	86.5 ± 5.8
HDL (mg dL^{-1})	58.8 ± 3.9	36.6 ± 5.1	46.9 ± 2.7	53.6 ± 2.7
LDL (mg dL^{-1})	74.2 ± 6.7	168.7 ± 11.8	88.1 ± 8.7	78.6 ± 5.5
Phospholipid (mg dL^{-1})	44.5 ± 3.5	24.1 ± 1.3	35.1 ± 2.5	41.3 ± 2.1

[a] Values are expressed as mean ± SEM ($n = 3$). $P > 0.05$ when compared to the normal group.

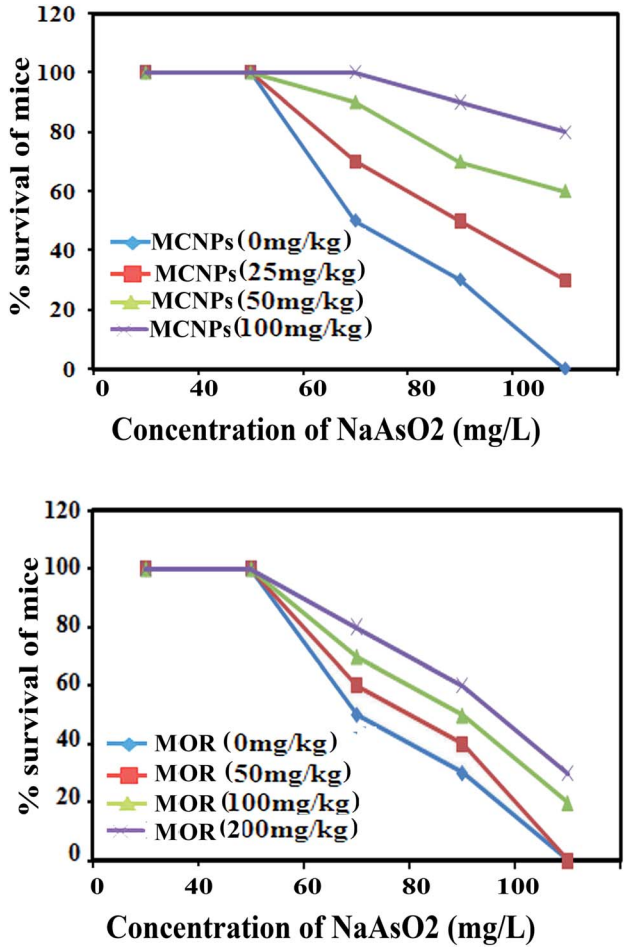

Fig. 3 Effect of different concentrations of MOR and MCNPs against 60 mg L^{-1} arsenic-induced mortality in mice on the indicated days. The percent survival of mice following oral treatment of (A) MCNPs (0, 25, 50, and 100 mg kg^{-1} bwt) and (B) MOR (0, 50, 100, and 200 mg kg^{-1} bwt) in mice on every alternate day from day 2 up to 30.

alteration in body weight, and the level of the blood parameters and kidney function markers (Table 1). Also, the higher serum level of LDL, TG and TC, and the low level of HDL were significantly altered following treatment with 50 mg kg^{-1} bwt MCNP and 200 mg kg^{-1} bwt of MOR (Table 1).

Effect of MOR and MCNPs on survival of mice against arsenic induced mortality and arsenic deposition in different organs

The therapeutic benefit of MOR and MCNPs was assessed by measuring its survival effect on arsenic induced mortality in a mouse model. Following treatment of 0 mg, 25 mg, 50 mg and 100 mg kg^{-1} of MCNPs, the survival of mice were (a) 0%, 30%, 60%, and 80% respectively on day 40, (b) 20%, 45%, 70% and 90% respectively on day 30, (c) 40%, 60%, 85%, and 100% respectively on day 20, and (d) 100% on day 10 against the mortality induced by 60 mg L^{-1} of arsenic exposed *via* drinking water (Fig. 3A). Similarly, the percent survival resulting from treatment of 0 mg, 50 mg, 100 mg and 200 mg kg^{-1} of MOR were (a) 0%, 0%, 15%, and 25% respectively on day 40, (b) 20%, 25%, 40% and 50% respectively on day 30, (c) 35%, 40%, 55%, and 70% respectively on day 20, and (d) 100% on day 10 (Fig. 3B).

Table 2 shows the effect of MOR and MCNP treatment on arsenic deposition in the liver, kidney, brain, lung, heart and skin. Exposure to arsenic resulted in a significant increase in the arsenic concentration in these organs. Arsenic deposition is found to be higher in the liver than any other organs. Administration of MCNPs and MOR lowered the amount of arsenic deposited in these organs (Table 2).

MCNPs suppress oxidative stress in the mouse liver

Treatment with MOR or MCNPs significantly prevented arsenic-induced ROS generation and increase of the MDA level (Fig. 4A and B). Fig. 4C shows the change in the ROS level as seen in the confocal microscopy study using DCFDA (green) and the change is the same as that shown in Fig. 4A.

MCNPs enhance the production of antioxidant factors in the mouse liver

Nrf2 activation induces phase II detoxifying enzymes such as glutathione (GSH), catalase (CAT), glutathione S-transferase (GST), hemeoxygenase-1 (HO-1), NAD(P)H:quinone oxidoreductase 1 (NQO1), glutathione peroxidase (GPx), *etc.* against oxidative stress. The SOD was up-regulated by MOR (200 mg kg^{-1}) and MCNPs (50 mg kg^{-1}) in arsenic exposed mice (Fig. 5A). Catalase and GSH levels were low in the arsenic group. It increased in the arsenic group receiving MCNPs (Fig. 5B and C). MCNP treatment increased the levels of nuclear Nrf2, GST, and GPx which were decreased due to arsenic exposure (Fig. 5D). Also, Fig. 5D shows that cytosolic Nrf2 and Keap1 markedly increased in the arsenic group which were lowered following MCNP treatment. Similar findings were observed in the levels of HO-1 and NQO1 (Fig. 5E). The effect of 50 mg kg^{-1} bwt MCNPs was the same as that of 200 mg kg^{-1} of MOR. This indicated that MCNPs have a strong antioxidant capacity against arsenic-induced liver injury.

Table 2 Arsenic deposition in different organs[a]

Arsenic concentration ins μg g^{-1} of tissue in 30 days						
	Liver	Kidney	Cerebellum	Lung	Heart	Skin
Arsenic, 40 mg L^{-1}	139.3 ± 6.3	25.7 ± 1.7	11.6 ± 0.47	12.6 ± 0.35	11.4 ± 0.66	4.2 ± 0.26
Arsenic + MOR (200 mg kg^{-1})	112.7 ± 6.5	17.3 ± 0.45	8.8 ± 0.21	8.9 ± 0.29	7.5 ± 0.41	1.3 ± 0.06
Arsenic + MCNP (50 mg kg^{-1})	45.6 ± 2.5	3.6 ± 0.42	0.82 ± 0.06	1.5 ± 0.04	1.8 ± 0.11	0

[a] Values are expressed as mean ± SEM ($n = 3$). $P > 0.05$ when compared to the normal group.

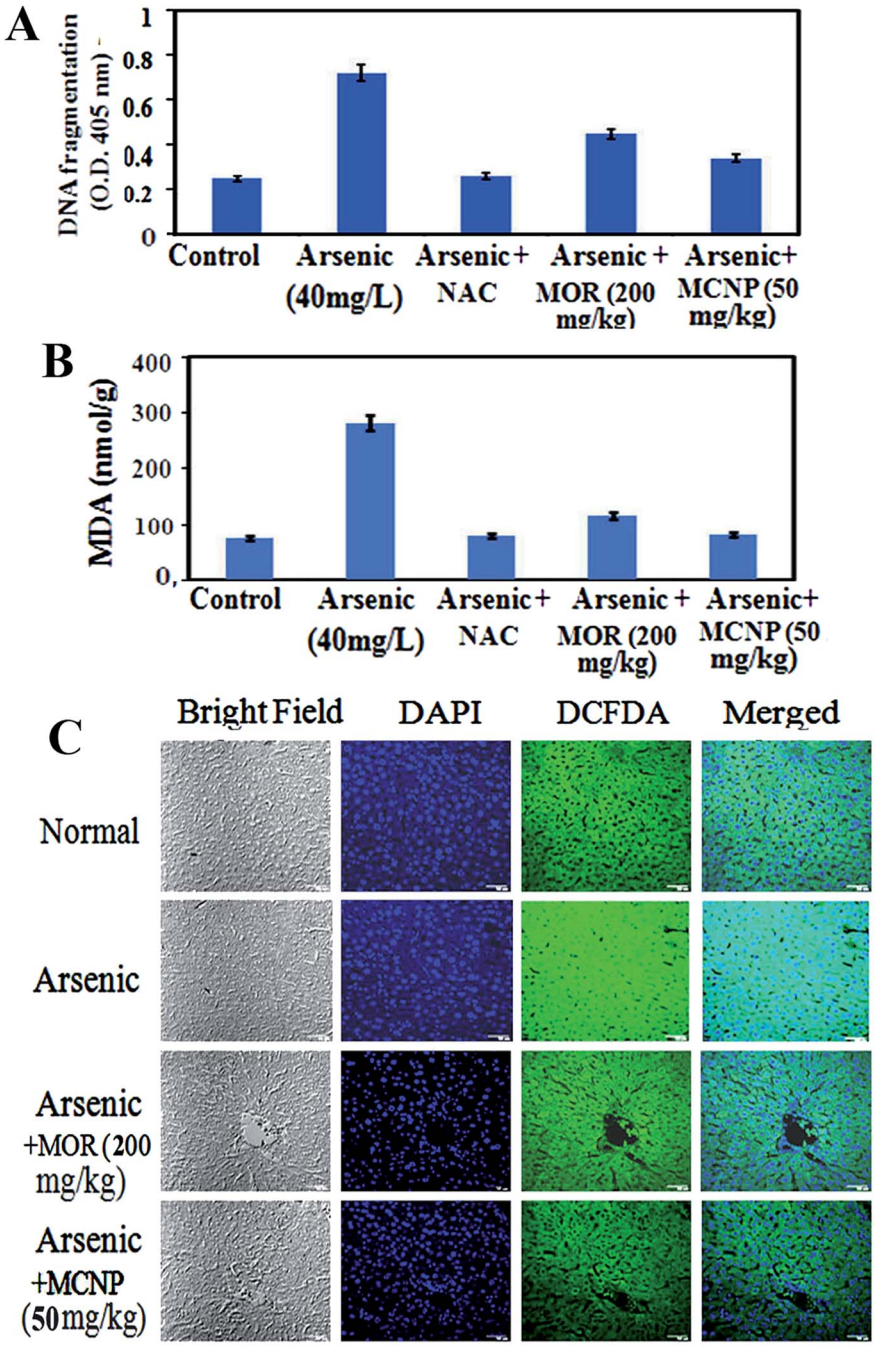

Fig. 4 Effect of MOR and MCNPs on ROS generation and the MDA level. Mice exposed to arsenic *via* drinking water were treated with MCNPs (50 mg kg^{-1} bwt) and MOR (200 mg kg^{-1} bwt) orally on every alternate day and the levels of (A) ROS and (B) MDA were determined. (C) ROS detection in liver tissues after staining with DAPI and DCFDA (green fluorescence) followed by fluorescence imaging using a confocal microscope.

MCNPs inhibit apoptosis and improve histology of the liver

To further investigate the role of MCNPs in As(III) – induced liver cell dysfunction, the expression of apoptosis related proteins was detected. Excessive ROS production by arsenic triggers cell death through apoptosis.[16] The apoptosis is associated with the activation of pro-apoptotic Bax/Bak, Bad, release of cytosolic cytochrome C, and apoptotic protease activating factor-1 (Apaf-1), stimulation of caspase-3 and caspase-9, activation of PUMA (p53 upregulated modulator of apoptosis) and DNA fragmentation.[17]

Arsenic mediated enhancement of DNA fragmentation, active caspase-3/caspase-9, and cytosolic cytochrome C were suppressed by MCNPs in the liver tissue lysate (Fig. 6A and B). Bax, Bak, Bad, Apaf-1, and PUMA were found to be suppressed in the liver tissue lysate of the arsenic + MOR and arsenic + MCNP groups in contrast to their higher level in the arsenic

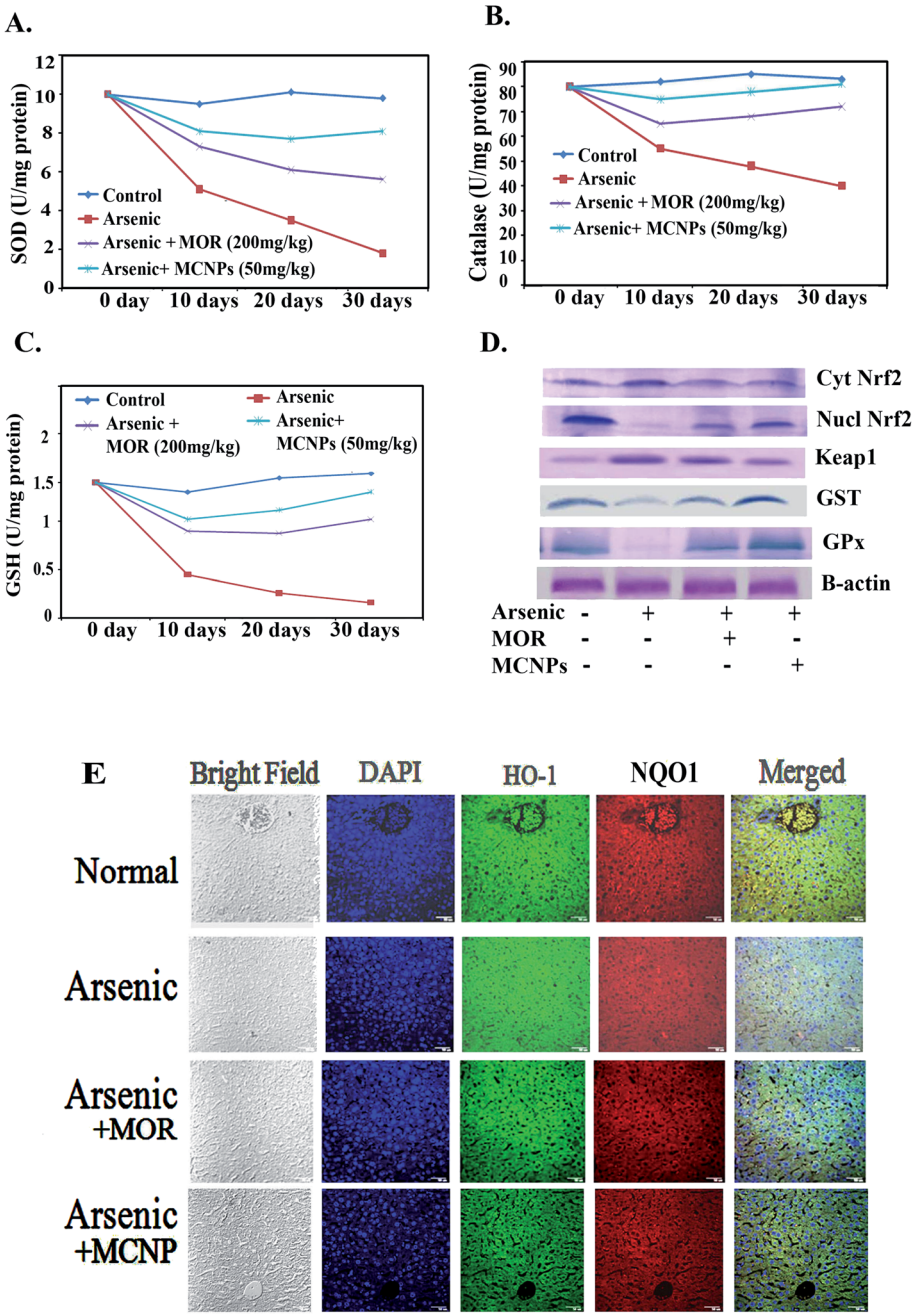

Fig. 5 Effect of MCNPs and MOR on antioxidant factors. Mice were orally treated with MCNPs (50 mg kg^{-1} bwt) and MOR (200 mg kg^{-1} bwt) during their exposure to arsenic. The levels of (A) SOD, (B) catalase and (C) GSH in the liver tissue lysate of arsenic were measured by using assay kits. (D) Shows the effect of MCNPs and MOR on protein expression of cytosolic Nrf2, nuclear Nrf2, Keap1, GST, and GPx (western blot analysis) in the liver tissue lysate. (E) Expression of HO-1 and NQO1 as seen in immunohistochemical analysis.

group. Anti-apoptotic protein Bcl-2 suppressed by arsenic was enhanced following the treatment of MOR and MCNP (Fig. 6C).

H&E staining of liver tissue sections was performed to evaluate the histopathological changes.

The livers of the normal, only MOR and MCNP treated groups showed undamaged hepatocytes in which normal looking sinusoids were lined by Kupffer cells whereas exposure to arsenic showed severe injury characterized by diffused Kupffer cells, vascular changes, and inflammatory cell infiltration (Fig. 6D). Treatment of mice with MOR and MCNPs during arsenic exposure showed minor or no hepatocellular damage, inflammatory cell infiltration, and no marked histopathological alterations were noticed. Treatment with MCNPs significantly alleviated chronic arsenic-induced deleterious effects.

MCNPs suppressed arsenic induced inflammatory responses

Dissociation of IkBα from NF-kB in the cytosol leads to its translocation into the (activation) nucleus resulting in

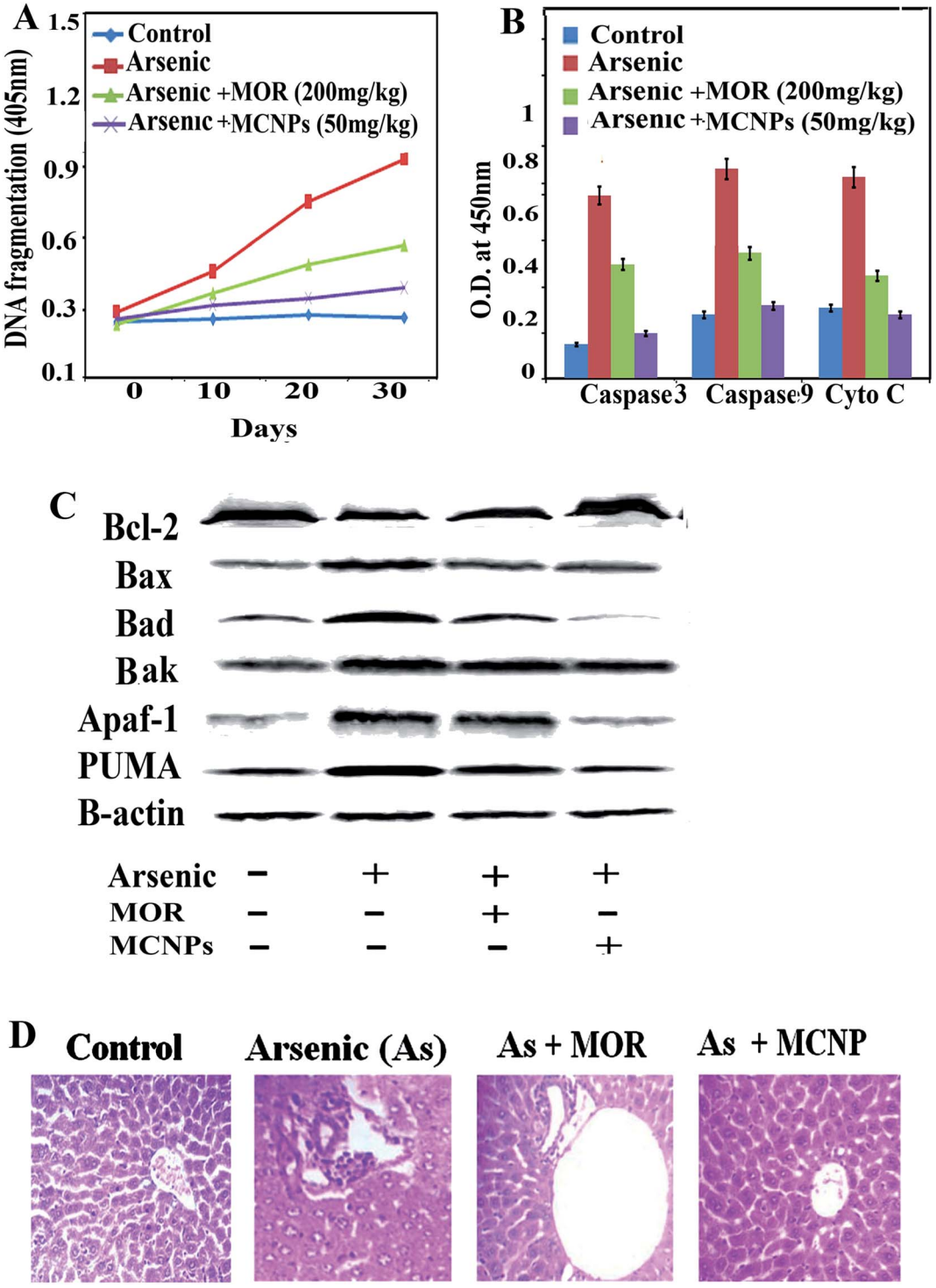

Fig. 6 Effect of MCNPs and MOR on liver tissue apoptosis and histology. (A) Level of DNA fragmentation obtained using a DNA fragmentation kit. (B) The level of active caspase-3, active caspase-9, and cytosolic cytochrome C obtained using respective colorimetric assay kits. (C) Shows the effect of MCNPs and MOR on the protein expression (western blot analysis) of Bcl-2, Bax, Bad, Bak, Apaf-1 and PUMA in mice exposed to arsenic. (D) Architecture of liver tissue section following treatment without or with MCNPs and MOR in arsenic exposed mice.

enhanced production of pro-inflammatory mediators.[18] During arsenic exposure, NF-kBp65 is highly activated with the release of a high level of inflammatory cytokines. Treatment of MOR and MCNPs attenuated the scale of these cytokines such as TNF-α, IL-1β and IL-6 elevated by arsenic (Fig. 7A). NF-kBp65 and NF-kBp50, both the subunits of NF-kB activated in arsenic exposed mice are suppressed following the treatment of MCNPs or MOR (Fig. 7B). Chronic arsenic exposure is also associated with the

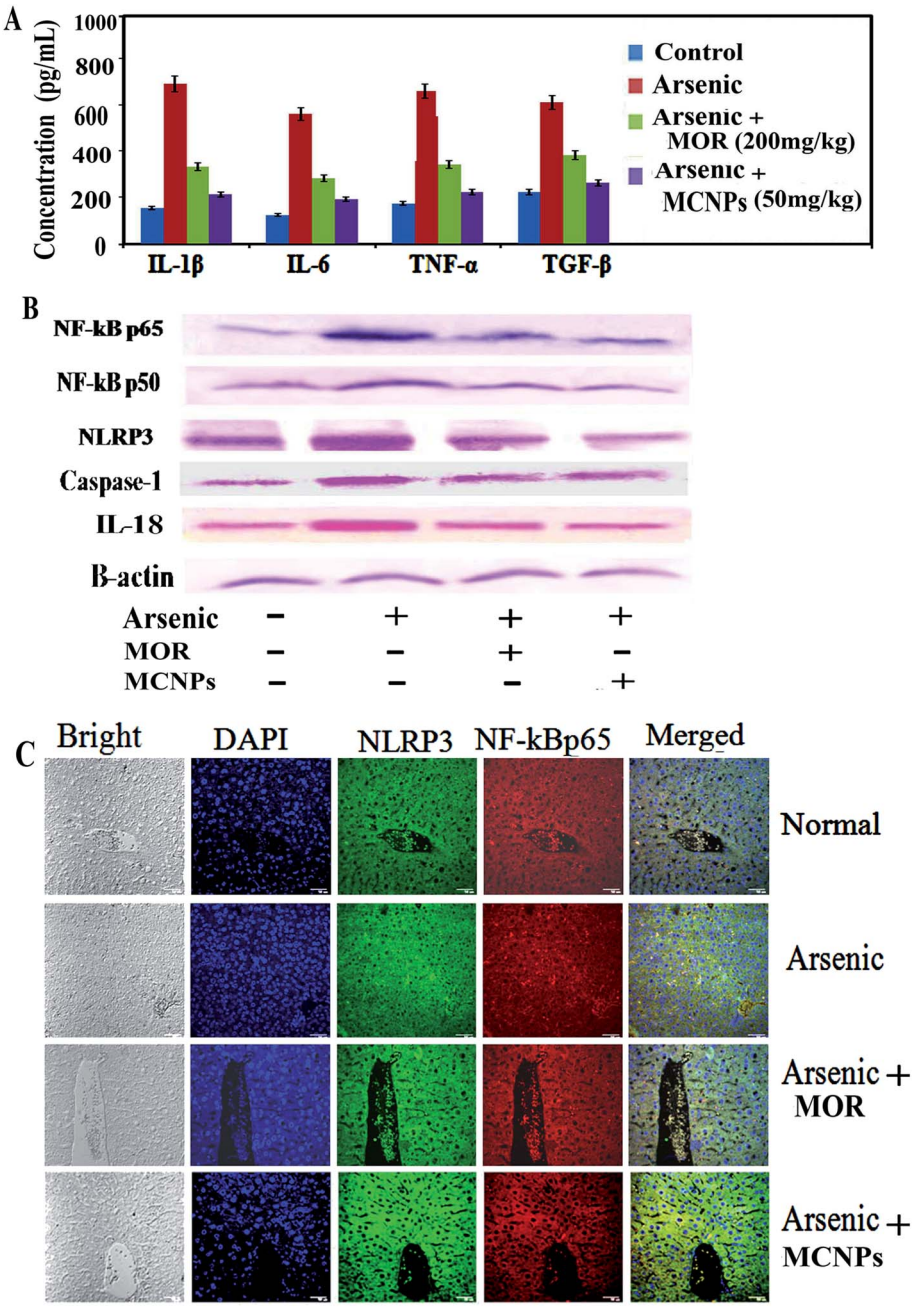

Fig. 7 Effect of MCNPs and MOR on the level of (A) TNF-α, IL-β, IL-6, and TGF-β in the liver tissue lysate of arsenic challenged mice as seen in ELISA analysis. Data show one of the three representative experiments ± SD. (B) Shows the effect of MCNPs and MOR on protein expression of nuclear NF-kBp65 and NF-kBp50, NLRP3, caspase-1, and IL-18 (western blot analysis). (C) Shows the expression of NF-kBp65and NLRP3(confocal images) in arsenic exposed mice.

activation of the NLRP3 inflammasome and the release of pro-inflammatory factors caspase-1, IL-1b and IL-8 which cause pyroptosis. MCNPs alleviated the level of the NLRP3 inflammasome that was elevated by arsenic and the level of caspase-1 and IL-8 in liver tissue (Fig. 7B). Downregulation of the expression of NF-kBp65 and NLRP3 by MOR and MCNPs in the liver tissue of arsenic exposed mice observed by confocal microscopy is shown in Fig. 7C.

Tissue distribution study of MCNPs in various organs

After oral administration of a single dose of MCNPs and MOR in mice for various time intervals, the content of free morin in the liver, spleen, lungs, kidneys, and serum were monitored by high-performance liquid chromatography (HPLC). As shown in Fig. 8A, the morin content from MCNPs showed different concentrations in the organs. Its highest concentration was found in the liver at 2 h that gradually decreased with time and

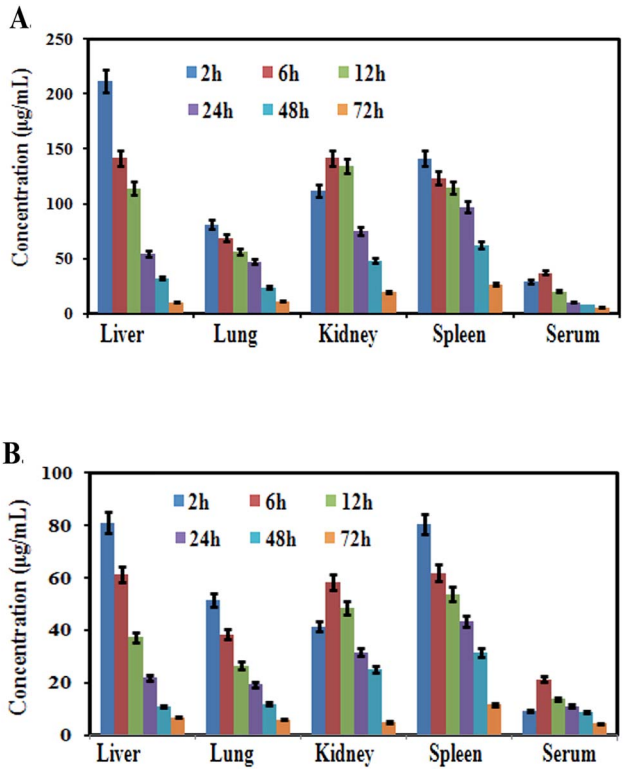

Fig. 8 Tissue distribution studies of MCNPs and MOR in various organs. The mean concentration of morin in the liver, lungs, kidneys, spleen, and serum at 2, 6, 12, 24, 48, and 72 h after oral administration of a single dose of (A) MCNPs and (B) MOR ($n = 3$, mean ± SD) in mice.

was low at 72 h. The order of the concentration of morin in different organs was liver > kidney ≥ spleen > lung > serum. Over time, the main trend of the concentration of morin in all organs was reduced slowly suggesting negligible or no accumulation in the tissues and a slow elimination of this compound. The amount of morin accumulated in the organs of free morin treated mice was about 4–5 times less compared to the MCNP treatment. The trend of reduction of the morin concentration in the organs was the same as that of MCNPs (Fig. 8B).

Discussion

The present study shows that arsenic exposure causes hepatic damage *via* elevation of liver function markers, alteration of lipid profiles, and increased arsenic deposition in organs with enhancement of ROS generation, inflammation and apoptosis. The supplementation of morin encapsulated chitosan (MCNPs) and morin (MOR) normalizes the anomalies caused by arsenic. The efficacy of MCNPs is higher than that of free MOR.

Arsenic pollution in India has become a menace to human health. One of the major complications that occur due to long term accumulation of arsenic is liver injury as it generates ROS like ethoxy, superoxide, hydroxyl, peroxyl and hydrogen peroxide radicals.[18] Oxidative stress induced lipid peroxidation causes many pathological events. An increased level of TG leads to diseases like diabetes mellitus, obesity, chronic renal disease, and cardiovascular disorders. ROS attack hepatocytes, stellate cells, Kupffer cells and their signaling mediators' interleukins, and growth factors finally leading to hepatic fibrosis and cirrhosis.[17] Treatment of liver disorders is expensive and has various side effects.[18] Therefore there is a shift towards an alternative system of medicine nowadays. Owing to the strong antioxidant and anti-inflammatory activities, polyphenols of plant and food origin exhibit a protective effect against various chronic diseases including liver disorder.[19] The hepatoprotective effect of polyphenols like silibinin/silymarin, quercetin, morin, genistein, naringenin, resveratrol, EGCG, curcumin, chlorogenic acid, and berberine have been reported.[20] There are also report of the hepatoprotective activity of the polyphenols ECGC, quercetin, lutein, grape seed extract, gallic acid and tannic acid against arsenic intoxification.[20] Antioxidant and hepatoprotective effects of the polyphenol morin against hepatic damage induced by different drugs and chemicals have been reported by several researchers.[21,22] The protective effects of curcumin, quercetin and resveratrol NPs against hepatic damage are well documented.[23,24] Chitosan NPs also show a promising protective role in the management of hepatic injury induced by acetaminophen, alcohol, diethylnitrosamine (DEN), CCl4, and concanavalin A.[25–28] In this respect the hepatoprotective activity of MCNPs against arsenic induced hepatotoxicity is quite justified. Improvement of normal liver architecture by MCNP treatment in arsenic exposed mice is in harmony with the previous report.[29,30]

This study indicates that MCNPs may work as a stronger antioxidant than free morin to ameliorate arsenic-induced hepatotoxicity caused by ROS generation. During arsenic exposure, the ROS level is highly enhanced and the level of antioxidant enzymes and anti-oxidant factors are lowered as reflected in increased ROS and MDA levels and decreased levels of SOD, catalase, GSH, nuclear Nrf2, HO-1 and NQO-1 in the liver tissue lysate. Many studies have reported that arsenic induced hepatic injury results from excessive oxidative stress and DNA damage.[2] MCNPs markedly inhibit DNA damage and hepatic injury. Thus, the protective effects of MCNPs against arsenic toxicity are reflected in their ability to suppress ROS/MDA and activate Nrf2 and its downstream anti-oxidant enzymes SOD, catalase, HO-1, GPx *etc.* A similar effect was seen with MOR. But its effect was much less than that of MCNPs. The findings of Hussein *et al.* and Tzankova *et al.* on hepatoprotective activity of quercetin and curcumin loaded nanoparticles through the enhancement of these antioxidants support our data.[29,31] Arsenic induced hepatic damage occurs through apoptosis.[32] Groups of pro-apoptotic proteins of the Bax family, apoptosis inducer initiator protease caspase-9 and effector protease caspase-3, and apoptosis triggering protein cytochrome C are activated and the anti-apoptotic Bcl-2 protein is suppressed in arsenic exposed mice.[33] Treatment of MCNPs prevented liver tissue damage by inhibiting apoptosis *via* alteration of the expression of the above proteins regulating apoptosis.

One hallmark of the inflammatory response is the production of proinflammatory cytokines TNF-α, IL-1β, and IL-6 *via* activation of NF-κB and/or inflammasome NLRP3.[34] These pro-

inflammatory factors aggravate further tissue damage that is triggered by arsenic mainly *via* its binding with the thiol groups of cellular proteins and ROS generation.[16] Enhanced expression of NF-κB and its target cytokines TNF-α, IL-1β, and IL-6 in liver tissue confirms arsenic induced hepatotoxicity. MCNPs attenuated the level of these inflammatory factors. There is evidence for protection against liver damage by morin through the inhibition of inflammation.[22] So our findings can be justified by these observations.

Some previous reports indicate that liver tissue can absorb particles up to 250 nm in size, and better internalization was shown by spherical-shaped NPs. [32]MCNPs were spherical and 124.5 nm in diameter, indicating the continuous release of MOR for 72 h. All the relevant functional groups of MOR were conserved in their chitosan-encapsulated forms. MCNPs showed marked inhibition (nearly 4 times higher) with respect to morin. Our data showed that the effect of MOR (100 mg kg^{-1}) is comparable to that of MCNPs (25 mg kg^{-1}). This could be due to the increase in water solubility, bioavailability and sustained drug release from the nanocomposites.

The architecture of the hepatic tissue of the control and MCNP treated mice along with arsenic was more or less similar, showing hepatocytes arranged in cords radiating from the central vein. They are polygonal cells with pale vesicular nuclei and prominent nucleoli. Blood sinusoids were found as a network between the plates of hepatocytes converging towards the central vein. Loss of cellular architecture, degeneration of hepatocytes, infiltration of inflammatory cells, and dilated sinusoidal and focal necrosis showed the damage of the liver in arsenic exposed mice (Fig. 6D). Some hepatocytes showed early signs of apoptosis with fragmented nuclei and hazy vacuolated cytoplasm. Apoptotic hepatocytes were also detected, showing nuclear and cytoplasmic condensation into deeply stained apoptotic bodies. When MCNPs were administered with arsenic, the liver sections appeared somewhat normal in histological architecture. Almost normal hepatocytes separated by clear sinusoids were observed. Loss of cellular architecture, degeneration of hepatocytes, infiltration of inflammatory cells, and dilated sinusoidal and focal necrosis showed the damage of the liver in arsenic treated mice as compared to normal mice. An improvement of regeneration was seen by the well-recovered hepatocytes separated by clear sinusoids in groups treated with MOR and MCNPs.

Recently, various nanoparticles have been employed to treat various inflammatory diseases and have shown successful results.[36] Polymeric nanoparticles sized 50 and 200 nm favors faster and more oral absorption, can efficiently be transported across the intestinal membrane, and mainly accumulate in the liver.[37] Small-sized nanoparticles (<5 nm) are filtered out by the kidneys. Sphere shaped nanoparticles are taken up by cells more readily than any other shape nanoparticles and have received significant attention. Natural polymers have gained popularity compared to the synthetic variety due to biodegradability, biocompatibility, and economic and environmental friendliness.[38]

Oral treatment of resveratrol, quercetin, curcumin and EGCG loaded polymeric nanoparticles shows higher water solubility, sustained release of the drug, better bioavailability and higher biodistribution efficacy compared to the pure drug.[27–29] Also, these nanoparticles can easily cross the intestinal barrier after their oral administration and therefore, it is effectively used for oral drug delivery. Polyphenol-loaded polymeric nanoparticles can easily pass through the membrane and be internalized by cells and provide better absorptivity in comparison with the pure drug.[38] Also, polymeric nanoparticles of polyphenols shows better anti-inflammatory and antioxidant effects than the free drug and they strongly inhibits apoptosis and lipid peroxidation.[35,38] These pieces of evidence strongly support the higher antioxidant, anti-inflammatory and anti-apoptotic effects of chitosan encapsulated morin nanoparticles than those of free morin as observed in our study.

Conclusion

Our study indicates that MCNPs showed a better protective effect than MOR against arsenic-induced hepatotoxicity in mice. The greater hepatoprotective activity of MCNPs can be explained by the increased solubility and bioavailability of MOR due to the formulation of chitosan nanoparticles. The antioxidant, anti-inflammatory and antiapoptotic activities can be considered as main factors responsible for the hepatoprotective effect of MCNPs. The results showed that MCNPs suppressed ROS formation and increased the antioxidant potential. MCNPs also ameliorated inflammatory responses and apoptosis. Therefore, MCNPs may represent a potential therapeutic option to prevent liver tissue injury induced by arsenic exposure.

Author contributions

Sanchaita Mondal – conceptualization, data curation, formal analysis, validation, visualization, writing original draft; Sujata Das – data curation, methodology, formal Analysis; Pradip Kumar Mahapatra – supervision; Krishna Das Saha – funding acquisition, investigation, resources, software, supervision.

Conflicts of interest

We wish to confirm that there are no known conflicts of interest associated with this publication and there has been no significant financial support for this work that could have influenced its outcome.

Acknowledgements

The research is supported by the DBT-NER and National Medicinal Plant Board, Ministry of AYUSH, Government of India. The authors are thankful to Mr T. Muruganandan, Dr Ramdhan Majhi, Mr Soumik Laha, Mr Binayak Pal and Smt. Banasri Das of the Central Instrumentation Facility, CSIR-Indian Institute of Chemical Biology for atomic force microscopy, HPLC, FT-IR, and confocal microscope facilities. The authors are very obliged to the Director of CSIR-IICB for providing the necessary support.

References

1 I. Palma-Lara, M. Martínez-Castillo, J. C. Quintana-Pérez, M. G. Arellano-Mendoza, F. Tamay-Cach, O. L. Valenzuela-Limón, E. A. García-Montalvo and A. Hernández-Zavala, Arsenic exposure: a public health problem leading to several cancers, *Regul. Toxicol. Pharmacol.*, 2020, **110**, 104539, DOI: 10.1016/j.yrtph.2019.104539.

2 K. Jomova, Z. Jenisova, M. Feszterova, S. Baros, J. Liska, D. Hudecova, C. J. Rhodes and M. Valko, Arsenic: toxicity, oxidative stress and human disease, *J. Appl. Toxicol.*, 2011 Mar, **31**(2), 95–107, DOI: 10.1002/jat.1649.

3 B. Li, X. Li, B. Zhu, X. Zhang, Y. Wang, Y. Xu, H. Wang, Y. Hou, Q. Zheng and G. Sun, Sodium arsenite induced reactive oxygen species generation, nuclear factor (erythroid-2 related) factor 2 activation, heme oxygenase-1 expression, and glutathione elevation in Chang human hepatocytes, *Environ. Toxicol.*, 2013 Jul, **28**(7), 401–410, DOI: 10.1002/tox.20731.

4 K. Renu, A. Saravanan, A. Elangovan, S. Ramesh, S. Annamalai, A. Namachivayam, P. Abel, H. Madhyastha, R. Madhyastha, M. Maruyama, V. Balachandar and A. V. Gopalakrishnan, An appraisal on molecular and biochemical signalling cascades during arsenic-induced hepatotoxicity, 2020, **260**:118438, DOI: 10.1016/j.lfs.2020.118438.

5 S. Zhao, T. Song, Y. Gu, Y. Zhang, S. Cao, Q. Miao, X. Zhang, H. Chen, Y. Gao, L. Zhang, Y. Han, H. Wang, J. Pu, L. Xie and Y. Ji, Hydrogen Sulfide Alleviates Liver Injury Through the S-Sulfhydrated-Kelch-Like ECH-Associated Protein 1/Nuclear Erythroid 2-Related Factor 2/Low-Density Lipoprotein Receptor-Related Protein 1 Pathway, *Hepatology*, 2021 Jan, **73**(1), 282–302, DOI: 10.1002/hep.31247.

6 F. Klibet, A. Boumendjel, M. Khiari, A. E. Feki, C. Abdennour and M. Messarah, Oxidative stress-related liver dysfunction by sodium arsenite: Alleviation by Pistacia lentiscus oil, *Pharm. Biol.*, 2016, **54**(2), 354–363, DOI: 10.3109/13880209.2015.1043562.

7 A. Singaravelu, K. Venkatachalam, R. L. Jayaraj, P. Jayabalan and S. Nadanam, Morin treatment for acute ethanol exposure in rats, *Biotech. Histochem.*, 2021 Apr, **96**(3), 230–241, DOI: 10.1080/10520295.2020.1785548.

8 J. Li, Y. Yang, E. Ning, Y. Peng and J. Zhang, Mechanisms of poor oral bioavailability of flavonoid Morin in rats: From physicochemical to biopharmaceutical evaluations, *Eur. J. Pharm. Sci.*, 2019 Feb 1, **128**, 290–298, DOI: 10.1016/j.ejps.2018.12.011.

9 M. Sasidharan, H. Zenibana, M. Nandi, A. Bhaumik and K. Nakashima, Synthesis of mesoporous hollow silica nanospheres using polymeric micelles as template and their application as a drug-delivery carrier, *Dalton Trans.*, 2013, **42**, 13381, DOI: 10.1039/c3dt51267c.

10 A. Modak, A. Kumar Barui, C. R. Patra and A. Bhaumik, A luminescent nanoporous hybrid material based drug delivery system showing excellent theranostics potential for cancer, *Chem. Commun.*, 2013, **49**, 7644, DOI: 10.1039/c3cc43487g.

11 R. Mahmoudi, M. T. Ardakani, B. H. Verdom, A. Bahgeri, H. Mohammad-Beigi, F. Aliakbari, Z. Salehpour, M. Alipour, S. Afrouz and B. Hassan, Chitosan nanoparticles containing *Physalis alkekengi-L* extract: preparation, optimization and their antioxidant activity, *Bull. Mater. Sci.*, 2019, **42**, 131, DOI: 10.1007/s12034-019-1815-3.

12 C. Pasha and B. Narayana, Determination of arsenic in environmental and biological samples using toluidine blue or safanine O by simple spectrophotometric method, *Bull. Environ. Contam. Toxicol.*, 2008, **81**, 47–51.

13 C. G. Fraga, B. E. Leibovitz and A. L. Tappel, Lipid peroxidation measured as thiobarbituric acid-reactive substances in tissue slices: characterization and comparison with homogenates and microsomes, *Free Radicals Biol. Med.*, 1988, **4**(3), 155–161, DOI: 10.1016/0891-5849(88)90023-8.

14 Y. Fu, X. Sun, L. Wang and S. Chen, Pharmacokinetics and Tissue Distribution Study of Pinosylvin in Rats by Ultra-High- Performance Liquid Chromatography Coupled with Linear Trap Quadrupole Orbitrap Mass Spectrometry, *Evidence-Based Complementary Altern. Med.*, 2018, **2018**, 4181084.

15 S. Mallicka, B. C. Pal and J. R. Vedasiromoni, Deepak Kumar, Krishna Das Saha, Corchorusin-D Directed Apoptosis of K562 Cells Occurs through Activation of Mitochondrial and Death Receptor Pathways and Suppression of AKT/PKB Pathway, *Cell. Physiol. Biochem.*, 2012, **30**(4), 915–926.

16 Y. Hu, L. Jin, B. Lou, R. Wu, G. Wang, C. Lu, H. Wang, J. Pi and Y. Xu, The Role of Reactive Oxygen Species in Arsenic Toxicity, *Biomolecules*, 2020, **10**, 240, DOI: 10.3390/biom10020240.

17 E. Ramos-Tovar and P. Muriel, Molecular Mechanisms That Link Oxidative Stress, Inflammation, and Fibrosis in the Liver, *Antioxidants*, 2020, **9**(12), 1279, DOI: 10.3390/antiox9121279.

18 B. Henry, Drug Pricing & Challenges to Hepatitis C Treatment Access, *J. Health Biomed. Law*, 2018, **14**, 265–283.Author manuscript; available in PMC 2018 Sep 24. J Health Biomed Law.

19 H. Cory, S. Passarelli, J. Szeto, M. Tamez and J. Mattei, The Role of Polyphenols in Human Health and Food Systems: A Mini-Review, *Front. Nutr.*, 2018, DOI: 10.3389/fnut.2018.00087.

20 S. Li, H. Y. Tan, N. Wang, F. Cheung, M. Hong and Y. Feng, The Potential and Action Mechanism of Polyphenols in the Treatment of Liver Diseases, *Oxid. Med. Cell. Longevity*, 2018, **2018**, 8394818, DOI: 10.1155/2018/8394818.

21 S. G. Shankari, K. Karthikesan, A. M. Jalaludeen and N. Ashokkumar, Hepatoprotective effect of morin on ethanol-induced hepatotoxicity in rats, *J. Basic Clin. Physiol. Pharmacol.*, 2010, **21**(4), 277–294, DOI: 10.1515/jbcpp.2010.21.4.277.

22 H. S. Lee, K.-H. Jung, S.-W. Hong, In-S. Park, C. Lee, H.-K. Han, D.-H. Lee and S.-S. Hong, Morin protects acute

liver damage by carbon tetrachloride (CCl(4)) in rat, *Arch. Pharmacal Res.*, 2008 Sep, **31**(9), 1160–1165, DOI: **10.1007/s12272-001-1283-5**.

23 M. I. Yousef, S. A. M. Omar, M. I. El-Guendi and L. A. Abdelmegid, Potential protective effects of quercetin and curcumin on paracetamol-induced histological changes, oxidative stress, impaired liver and kidney functions and haematotoxicity in rat, *Food Chem. Toxicol.*, 2010, **48**(11), 3246–3261, DOI: **10.1016/j.fct.2010.08.034**.

24 N. M. Al-Baqami and R. Z. Hamza, Protective Effect of Resveratrol against Hepatotoxicity of Cadmium in Male Rats: Antioxidant and Histopathological Approaches, *Coatings*, 2021, **11**(5), 594, DOI: **10.3390/coatings11050594**.

25 E. Ozcelik, S. Uslu, N. Erkasap and H. Karimi, Protective effect of chitosan treatment against acetaminophen-induced hepatotoxicity, *Kaohsiung J. Med. Sci.*, 2014, **30**(6), 286–290, DOI: **10.1016/j.kjms.2014.02.003**.

26 M. Ahmed Abdelhakim, M. S. Radwan and A. H. Rady, Chitosan Nanoparticles as Hepato-protective agent against Alcohol and Fatty Diet Stress in rats, *Biochem. Int.*, 2017, **4**(1), 5–10.

27 K. Bai, B. Hong, J. He and W. Huang, Antioxidant Capacity and Hepatoprotective Role of Chitosan-Stabilized Selenium Nanoparticles in Concanavalin A-Induced Liver Injury in Mice., *Nutrients*, 2020, **12**(3), 857, DOI: **10.3390/nu12030857**.

28 E. Ozcelik, S. Uslu, N. Erkasap and H. Karimkhani, Protective effect of chitosan treatment against acetaminophen-induced hepatotoxicity, *Kaohsiung J. Med. Sci.*, 2014, **30**(6), 286–290, DOI: **10.1016/j.kjms.2014.02.003**.

29 V. Tzankova, D. Aluani, M. Kondeva-Burdina, Y. Yordanov, F. Odzhakov and A. Apostolov, Hepatoprotective and antioxidant activity of quercetin loaded chitosan/alginate particles *in vitro* and *in vivo* in a model of paracetamol-induced toxicity, *Biomed. Pharmacother.*, 2017, **92**, 569–579, DOI: **10.1016/j.biopha.2017.05.008**.

30 W. Teng, L. Zhao, S. Yang, C. Zhang, M. Liu, J. Luo, J. Jin, M. Zhang, C. Bao, D. Li, W. Xiong, Y. Li and F. Ren, The hepatic-targeted, resveratrol loaded nanoparticles for relief of high fat diet-induced nonalcoholic fatty liver disease, *J. Controlled Release*, 2019, **307**, 139–149, DOI: **10.1016/j.jconrel.2019.06.023**.

31 R. M. Hussein, M. A. Kandeil, N. A. Mohammed and R. A. Khallaf, Evaluation of the hepatoprotective effect of curcumin-loaded solid lipid nanoparticles against paracetamol overdose toxicity, Role of inducible nitric oxide synthase, *J. Liposome Res.*, 2022, 1–11, DOI: **10.1080/08982104.2022.2032737**.

32 A. Santra, A. Chowdhury, S. Ghatak, A. Biswas and G. K. Dhali, Arsenic induces apoptosis in mouse liver is mitochondria dependent and is abrogated by N-acetylcysteine, *Toxicol. Appl. Pharmacol.*, 2007 Apr 15, **220**(2), 146–155, DOI: **10.1016/j.taap.2006.12.029**.

33 S. elmore, Apoptosis: A Review of Programmed Cell Death, *Toxicol. Pathol.*, 2007, **35**(4), 495–516, DOI: **10.1080/01926230701320337**.

34 H. Kawaratani, T. Tsujimoto, A. Douhara, *et al.*, The effect of inflammatory cytokines in alcoholic liver disease, *Mediators Inflammation*, 2013, 495156.

35 W. Huang and C. Zhang, Tuning the size of poly(lactic-co-glycolic acid) (PLGA) nanoparticles fabricated by nanoprecipitation, *Biotechnol. J.*, 2018, **13**(1), 700203.

36 P. Rajitha, D. Gopinath, R. Biswas, M. Sabitha and R. Jayakumar, Chitosan nanoparticles in drug therapy of infectious and inflammatory diseases, *Expert Opin. Drug Deliv.*, 2016, **13**(8), 1177–1194, DOI: **10.1080/17425247.2016.1178232**.

37 H. He, Y. Xie, Y. Lv, J. Qi, X. Dong, W. Zhao, W. Wu and Y. Lu, Bioimaging of Intact Polycaprolactone Nanoparticles Using Aggregation-Caused Quenching Probes: Size-Dependent Translocation *via* Oral Delivery, *Adv. Healthcare Mater.*, 2018, **7**(22), e1800711, DOI: **10.1002/adhm.201800711**.

38 A. Kumari, S. K. Yadav and S. C. Yadav, Biodegradable polymeric nanoparticles based drug delivery systems, *Colloids Surf., B*, 2010, **75**(1), 1–18, DOI: **10.1016/j.colsurfb.2009.09.001**.